Cellulose-Based Fibers from Liquid Crystalline Solutions. III. Processing and Morphology of Cellulose and Cellulose Hexanoate Esters

VIPUL DAVÉ and WOLFGANG G. GLASSER*

Department of Wood Science and Forest Products; and Biobased Materials Center, Polymer Materials and Interfaces Laboratory, Virginia Polytechnic Institute and State University, Blacksburg, Virginia 24061

SYNOPSIS

Cellulose and a cellulose hexanoate ester (DS 0.69) exhibited liquid crystalline behavior in dimethylacetamide/lithium chloride and dimethylacetamide, respectively. The experimentally observed critical volume fraction (V_p^c) of cellulose was lower than that predicted by Flory's theory, whereas the experimental and theoretical values of V_p^c were within 70% of prediction for cellulose hexanoate. The V_p^c value obtained for cellulose hexanoate was lower than that previously reported for cellulose acetate butyrate with a maximum degree of butyration (CAB-3). This indicates that bulky substituents may lower V_p^c values. Fibers were spun from isotropic and anisotropic solutions of cellulose and cellulose hexanoate by a dry jet/wet spinning method. There was an increase in mechanical properties through the isotropic to anisotropic transition with moduli reaching 152 g/d (20.8 GPa) for cellulose fibers. The formation of cellulose fibers with high modulus at large extrusion rates and large takeup speeds (draw ratio) is explained with molecular organization prior to coagulation. This unexpected enhancement is attributed to the air gap that exists in the dry jet/wet spinning process. Similar improvements were not observed for cellulose hexanoate fibers. This is explained with incomplete development of liquid crystalline structure at the solution concentrations from which the fibers were spun.

INTRODUCTION

Cellulosic fibers (rayon) have been manufactured by the viscose process for almost a century. However, slow extrusion speeds, high pollution, high-energy consumption, and high investment costs have made the process uncompetitive. Research in the area of liquid crystal formation of cellulose in new solvent systems has been primarily driven by the aspiration to develop new nonpolluting processes to produce regenerated cellulose fibers. Since cellulose is the most abundant renewable organic raw material, it can replace petrochemicals. Because of its complex morphology of crystalline regions and hydrogen bonding, cellulose is difficult to dissolve in common solvents. Indirect solvent systems such as nitrogen tetroxide/dimethyl formamide or dimethyl sulfoxide,[1,2] paraformaldehyde/dimethyl sulfoxide,[3] chloral/dimethyl formamide/pyridine,[4] and urea/sodium hydroxide[5] form cellulose derivatives during the dissolution of cellulose, at least temporarily. Direct solvent systems may form a complex with cellulose, but no new covalent bonds are formed and cellulose maintains its original chemical structure. The dissolution process, byproduct control, and solvent recovery make direct solvent systems superior to their indirect counterparts for fiber spinning. A detailed review was published on different solvent systems of unmodified cellulose.[6] Only a brief summary of liquid crystalline studies of cellulose solutions in direct solvent systems is presented here.

Graenacher and Sallman[7] first discovered that a family of tertiary amine oxides is capable of dissolving cellulose. This was rediscovered by Johnson 30 years later.[8] The detailed mechanism of dissolution and fiber spinning of cellulose from this sol-

* To whom correspondence should be addressed.

Journal of Applied Polymer Science, Vol. 48, 683–699 (1993)
 CCC 0021-8995/93/040683-17

vent system was reported by investigators at American Enka.[9–14] The physical properties of these fibers were comparable to rayon fibers.

Chanzy et al.[15] were the first to report the formation of fibers from lyotropic mesophase of cellulose in the mixture of *N*-methylmorpholine *N*-oxide (MMNO) and water. The anisotropy depended on temperature of the solution (> 90°C), concentration of cellulose (> 20% [w/w]), mole ratio of water/anhydrous MMNO (< 1), and degree of polymerization of the dissolved cellulose. Structural and molecular characterization of MMNO in its anhydrous and monohydrate states was undertaken to investigate the basic geometry and conformation of MMNO and the nature of its interactions with water molecules.[16–18] Detailed investigations have been carried out on limiting viscosity number-molecular weight relationship,[19] rheology,[20,21] swelling,[22] crystallization,[23] phase behavior,[24] and fiber spinning[25–27] of cellulose in MMNO. Modulus and tenacity of dry jet/wet spun fibers were 21 and 0.5 GPa, respectively, from cellulose with DP = 600.[27] These fibers are in the process of commercialization under the tradename of Tencel by Courtaulds. MMNO was also utilized to prepare solutions from numerous polysaccharides (except chitin), and most of them formed anisotropic solutions.[28]

The highest cellulose concentrations achieved for this solvent system were 55% (w/w) for microcrystalline cellulose (DP 35) and 30–35% (w/w) for cellulose with DP 600–1000. It is recommended that a stabilizer such as *n*-propyl gallate be added to the solution to reduce cellulose degradation. High processing temperatures appear to be the limitation for spinning fibers from this system.

Patel and Gilbert showed lyotropic mesophase formation of cellulose in mixtures of trifluoroacetic acid (TFA) and chlorinated alkanes at room temperature.[29] The mesophase was identified to be cholesteric, and this is expected from the chirality of cellulose. An anisotropic phase was observed in 4% (w/w) solutions of Whatman cellulose in TFA–CH_2Cl_2 (70 : 30 v/v).[30] Degradation of cellulose occurred in TFA–CH_2Cl_2, presumably due to the attack of TFA at the glycosidic linkages, and the rate of degradation decreased with decreasing TFA/CH_2Cl_2 ratio.[30] There are no reports of fiber spinning from this solvent system. A number of Russian workers studied the cellulose–TFA and cellulose–TFA–$ClCH_2CH_2Cl$ systems[31–33] and prepared solutions up to 20% (w/w) concentration. Dissolution occurred without cellulose modification or oxidative degradation with little or no trifluoroacetylation of cellulose.[30,31]

Although first reported by Scherer in 1931,[34] the ammonia/ammonium thiocyanate solvent system for cellulose was systematically studied only recently by Hudson and Cuculo.[35–37] This solvent system is relatively nontoxic; it causes little or no degradation of cellulose, and the dissolution procedure is simple and safe. A detailed coagulation study for this solvent system was done to understand the fiber-forming ability of cellulose under various conditions.[38–40] A cellulose with DP 210 formed a cholesteric phase at 3.5% (w/v) and a nematic phase at 8–16% (w/v) at 25°C in a solvent containing 75.5% (w/w) ammonium thiocyanate and 24.5% (w/w) ammonia.[41] This type of lyotropic system makes it possible to selectively produce cellulose mesophases in either the cholesteric or nematic phase. Fibers spun from nematic cellulose solutions by the dry jet/wet spinning method had modulus and tenacity values of 44 and 0.98 g/d (DP 210) and of 167 and 3.4 g/d (DP 765), respectively.[41]

McCormick showed[42] that dimethylacetamide (DMAc)/lithium chloride (LiCl) is a good solvent system for cellulose, and he and his associates demonstrated the utility of this system for synthesizing various cellulose derivatives.[42,43] Solution studies of cellulose and the formation of cholesteric mesophase order were reported in this system by McCormick et al.[44,45] followed by Ciferri and co-workers.[46] Turbak et al. also studied the dissolution process and were first to describe fiber spinning of cellulose in this solvent system.[47] A critical aspect of this system is the necessity of activating the cellulose prior to dissolution. Maximum cellulose concentration achieved was 16% (w/w) with DP of 550.[47] LiCl–DMAc does not degrade or react with cellulose,[48] but it does form a complex with the hydroxyl groups on the cellulose backbone that results in its dissolution.[48,49] A pure anisotropic phase was not observed due to solubility limits. This prevents attainment of complete anisotropy. Bianchi et al.[50] reported on wet spun fibers from isotropic and anisotropic solutions of cellulose (DP 290) in LiCl (7.8%)/DMAc. Wet spinning involved the processing of solutions without an air gap. The fiber properties increased through the isotropic–anisotropic transition with modulus and tenacity values reaching 161 g/d (22 GPa) and 2.5 g/d (0.35 GPa), respectively.

Previously,[51] we established that solution anisotropy can be reached at increasingly lower concentrations if cellulose esters possess substituent groups that are increasingly large and bulky. This study is to further examine a cellulose derivative with an unusually large substituent (i.e., hexanoate) so as to test whether this principle applies in general.

The objectives of this study are to investigate the rheological and morphological properties of liquid crystalline solutions of cellulose and cellulose hexanoate and to establish structure–property relationships of fibers spun from isotropic and anisotropic solutions of cellulose and cellulose hexanoate by the dry jet/wet spinning process.

EXPERIMENTAL

I. Materials

Whatman CF-11 cellulose powder was used as received. Cellulose hexanoate was prepared in our laboratory by the acylation of Whatman cellulose in the homogeneous phase (3% DMAc/LiCl-9%) with hexanoic anhydride using 4-pyrrolidinopyridine (PP) as catalyst.[52] Reagent-grade DMAc and LiCl was used as received.

II. Methods

1. Determination of Molecular Parameters

Carbanilate derivatives of cellulose and cellulose hexanoate were prepared[53] to make solutions in HPLC-grade tetrahydrofuran (THF). The molecular parameters, like molecular weight, degree of polymerization (*DP*), intrinsic viscosity, and Mark–Houwink–Sakurda (MHS) constants, were determined using gel permeation chromatography with a differential viscosity detector (Viscotek Model No. 100) and a differential refractive index (concentration) detector (Waters 410) in sequence. All the calculations were based on a universal calibration curve.

2. Preparation of Solutions

Solutions of cellulose were prepared in DMAc/LiCl following the method described by Turbak et al.[47] with which complete dissolution was better achieved than with the method reported by McCormick and Chen.[54] Weighed amounts of DMAc were added to a weighed amount of cellulose that had been soaked in DMAc for 3 days. The mixture was heated to reflux temperature (approximately 165°C) for 20–30 min while being mechanically stirred under nitrogen atmosphere. The mixture was allowed to cool to about 100°C, and a weighed amount of LiCl was added under steady stirring. The mixture was stirred for about 30 min at 80°C before it was allowed to gradually cool to room temperature. Stirring was continued for about 20 h at room temperature. The cooled solution was slightly brown. Polymer concentration, C_p, given as grams of cellulose per 100 g of ternary solution (cellulose, DMAc, and LiCl), varied between 6.5 and 13.5%. Salt concentration, C_s, given as grams of LiCl per 100 g of binary solution (DMAc and LiCl) was kept at 7.8% for all solutions.

A complete range of solutions (5–40% [w/w]) were prepared by mechanically mixing known weights of cellulose hexanoate with DMAc at ambient temperature. LiCl was not required for these solutions.

The solutions were allowed to equilibrate for 2 weeks prior to analysis. Although this is excessive from a practical standpoint, extreme care was taken to treat the solutions similarly so that relative aging effects were constant for all of them.

3. Viscosity Measurements

Viscosity measurements of the solutions below 6.5 and 15% (w/w) concentration for cellulose and cellulose hexanoate, respectively, were made at 25°C using a Wells-Brookfield Cone/Plate Viscometer at different cone rotation speeds. A Rheometrics Mechanical Spectrometer (RMS 800) was used to determine the rheological properties of 15% (w/w) and higher concentrated solutions of cellulose hexanoate and all the other cellulose solutions. The solutions were placed in a parallel-disk geometry. The dynamic mechanical properties were measured at 26°C using a strain amplitude of 25% of the value at which the respective sample showed viscoelasticity. The frequency ranged from 0.1 to 100.0 rad/s.

4. Polarized Optical Microscopy

Polarized optical microscopy was performed with a Zeiss Axioplan Universal Microscope. Small amounts of cellulose and cellulose hexanoate solutions were placed between the microscope slide and coverslip, and these were examined for birefringence between the cross polarizers of the microscope at room temperature.

5. Fiber Spinning

Continuous fibers were processed from a single hole with a capillary diameter of 0.3 mm and using the dry jet/wet spinning method described in our earlier publication.[55] The flow rate of the solutions was varied between 0.4 and 3 cm^3/min by the extrusion pump. The fibers were wound on the spools at takeup speeds varying from 11 to 46 m/min. The air gap was about 1 in. Water was used as the coagulant at approximately 30°C. The fiber-wound spools were immersed in beakers containing water for 8 h and

were allowed to air-dry for about 8–10 h. The fibers were further vacuum-dried for 24 h at approximately 50°C. No postspinning treatments (thermal or mechanical) were performed.

6. Fiber Diameter

Fiber diameter (D) was determined by a Nikon UM-2 Measurescope equipped with a Quadra-Chek III attachment. The diameter was generally constant along an extended length of the fiber. The reported D value is the average of three to four measurements along the fiber length.

7. Mechanical Properties

The mechanical properties of the fibers were determined on an Instron 1130 Test Instrument following the procedure of ASTM standard D3822. Tests were conducted at room temperature and 67% relative humidity with 1 in. gauge length at a strain rate of 0.2 in./min. Single fibers were used for cellulose and cellulose hexanoate during testing. Linear density varied between 48 and 270 denier for cellulose hexanoate fibers and between 36 and 180 denier for cellulose fibers. The values of initial modulus (E), breaking tenacity (σ_b), breaking toughness (BT), and elongation at break (ϵ_b) were the average of 6–10 measurements.

8. Scanning Electron Microscopy

The fibers were examined on a JEOL JSM-35C scanning electron microscope with an accelerating voltage of 15 kV. Fracture surfaces were formed in liquid nitrogen. The fibers were mounted on aluminum specimen mounts (EMSL) with an angle of 45°. The fibers were coated at the bottom by Ladd Silver Conducting Paint and then sputter-coated by pure gold for 1 min (thickness about 9 nm) in an SPI Sputter Coater.

RESULTS AND DISCUSSION

Table I summarizes the chemical and molecular characteristics of the carbanilated derivatives of cellulose and cellulose hexanoate employed in this study. The degree of substitution (DS) of hexanoic groups (DS_{HEX}) was 0.69 as evaluated by proton NMR spectroscopy.[52] Unsubstituted hydroxyl groups (DS_{OH} = 2.31) in cellulose hexanoate were derivatized by the carbanilate groups to prepare solutions in THF for molecular weight determination. The DP_n of cellulose and cellulose hexanoate was 212 and 190, respectively. It should be noted that the MHS constant "a" was lower than expected for unsubstituted cellulose (i.e., 0.83). This is due to the bulky carbanilate groups.

Table I Chemical and Molecular Characteristics of Carbanilated Derivatives of Cellulose and Cellulose Hexanoate

	Cellulose Tricarbanilate	Carbanilated Cellulose Hexanoate
DS_{CAR}	3.0	2.31
DS_{HEX}[a]	0	0.69
$\langle M_n \rangle (\times 10^5)$	1.1	0.95
$\langle M_w \rangle (\times 10^5)$	1.8	1.4
DP_n	212	190
MHS constant (a)[b]	0.83	0.86
Intrinsic viscosity (dL/g)	1.34	1.05
Log K	−4.19	−4.36

[a] Determined by H-NMR spectroscopy.
[b] Mark Houwink Sakurada exponential factor.

I. Dynamic Viscoelastic Properties

1. Cellulose

The relationship between dynamic shear viscosity and concentration of cellulose solutions at different shear rates or frequencies (applying the Cox–Merz rule[56]) is demonstrated in Figure 1. The dynamic viscosity decreases and then increases at higher concentrations. The drop in viscosity after 7% (w/w) concentration is due to the onset of liquid crystalline behavior of the cellulose solutions. Seven percent (w/w) concentration is considered as the critical concentration value (C'_p) beyond which cellulose solutions exhibit liquid crystalline behavior in DMAc/LiCl. This value corresponds to V^c_p = 0.044. This drop in viscosity was not observed for cellulose solutions in DMAc/LiCl by McCormick et al.[44] or in TFA–CH_2Cl_2 by Gilbert and coworkers[30]; it was, however, reported for cellulose solutions in MMNO as a function of temperature.[20] To our knowledge, the observation of a critical concentration value by rheological measurements with cellulose solutions in DMAc/LiCl has never been reported before. The drop in viscosity is observed at constant concentration. This indicates that dynamic shear does not drive the thermodynamic transition of the anisotropic phase to a different concentration.

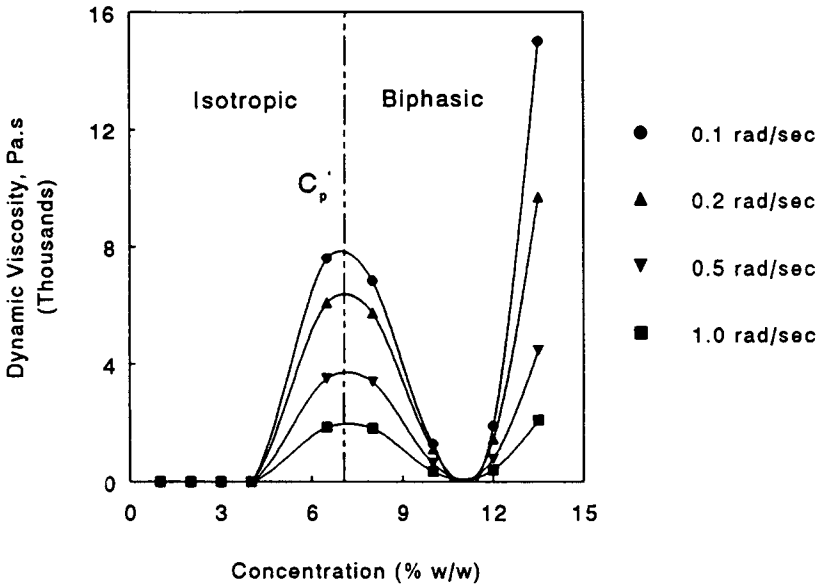

Figure 1 Dynamic viscosity vs. concentration of cellulose solutions in DMAc/LiCl at different frequencies.

At higher concentrations (i.e., above 12% [w/w]), the viscosity is seen to increase again. A similar rise in viscosity for cellulose solutions was universally observed by previous investigators.[30,44] Based on the phase diagram of cellulose in DMAc/LiCl, Ciferri and co-workers[46] showed that the cholesteric mesophase forms in the proximity of the limit of solubility. Therefore, the formation of a liquid crystalline phase represents a metastable condition that is closely associated with crystallization.[49] Consequently, the viscosity increases again at higher solution concentration. The viscosity of the solutions decreases with an increase in shear rate, and this confirms shear thinning behavior.

The relationship of dynamic elastic modulus (G') and dynamic loss modulus (G'') and concentration at different frequencies is shown in Figures 2 and 3, respectively. The feature of the concentration dependence of G' and G'' is identical to that seen for the dynamic viscosity, i.e., after the solution becomes liquid crystalline, G' and G'' decrease before increasing again at higher concentration. Similar to any viscoelastic material, G' increases with increasing frequency. G'' rises with frequency and does not fall even though the solutions are liquid crystalline. This shows that the damping characteristics of liquid crystalline solutions are higher than those of isotropic solutions. These results reveal that liquid crystalline cellulose solutions are viscoelastic in nature.

2. *Cellulose Hexanoate*

The relationship between dynamic shear viscosity and concentration of cellulose hexanoate solutions at different frequencies is shown in Figure 4. The viscosity increases with concentration and decreases with frequency. The expected decrease in viscosity at some critical concentration is not observed, and this is in contrast to typical polymer liquid crystalline solutions.

The relationships between dynamic elastic modulus (G') and dynamic loss modulus (G'') and concentration at different frequencies are shown in Figures 5 and 6, respectively. The characteristics of the concentration dependence of G' and G'' are the same as those observed for the dynamic viscosity. Similar trends were observed for cellulose solutions at higher concentrations (i.e., above 12%).

II. Polarized Optical Microscopy

1. *Cellulose*

Figure 7(a)–(c) shows the photomicrographs of 10% (w/w), 12% (w/w), and 13.5% (w/w) cellulose solutions, respectively. An increase in birefringence was observed as the solution concentration increased. Solutions below 10% (w/w) were isotropic. By contrast, the onset of liquid crystalline behavior by rheological observations was at 7% (w/w). Lyotropic mesophases of cellulose in DMAc/LiCl were

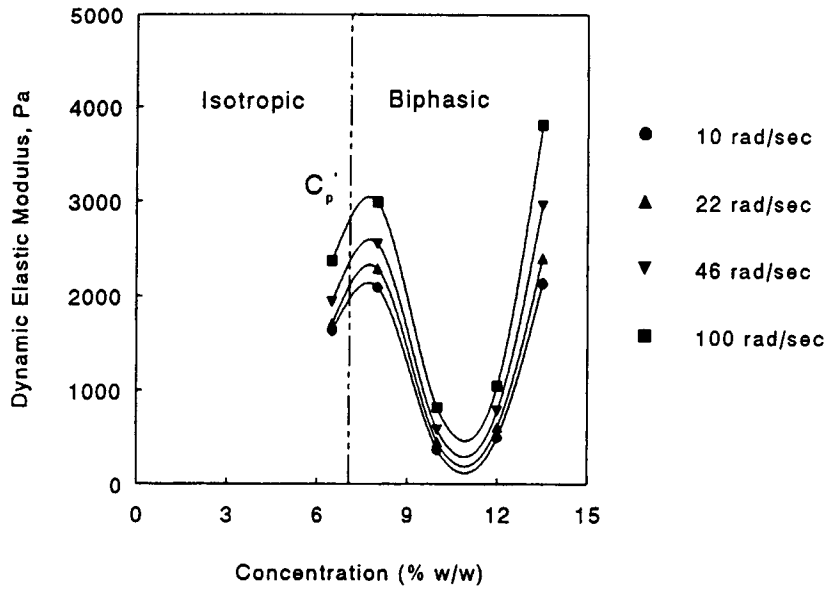

Figure 2 Dynamic elastic modulus vs. concentration of cellulose solutions in DMAc/LiCl at different frequencies.

reported to occur (by microscopy) at 11% (w/w) (DP 288) and 10% (w/w) concentrations by Ciferri and co-workers[46] and McCormick et al.,[44] respectively. These values are in overall agreement, and rheological measurements must be suspected to be more sensitive to the onset of molecular organization than is optical microscopy in this particular case.

2. *Cellulose Hexanoate*

Figure 8(a)–(d) are photomicrographs of 25% (w/w), 30% (w/w), 35% (w/w), and 40% (w/w) cellulose hexanoate solutions, respectively. The onset of liquid crystallinity is detected at approximately 25% (w/w). The solution becomes anisotropic at

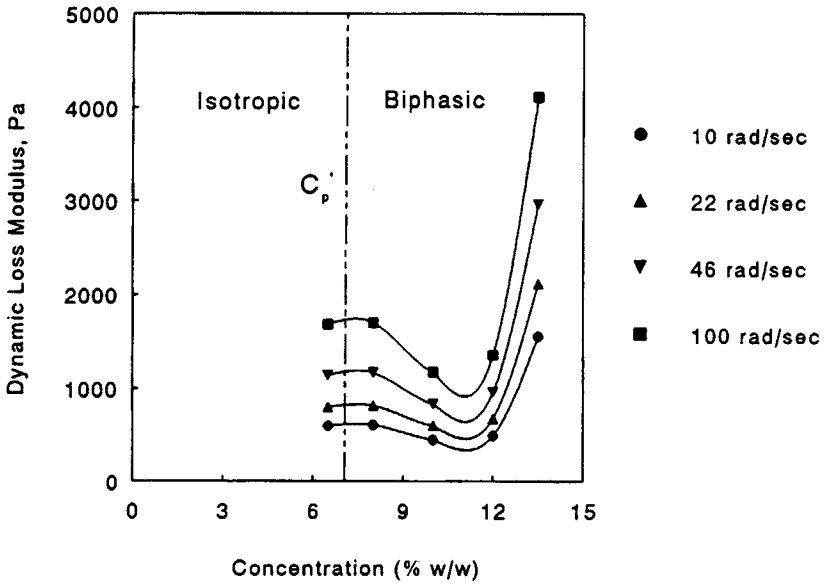

Figure 3 Dynamic loss modulus vs. concentration of cellulose solutions in DMAc/LiCl at different frequencies.

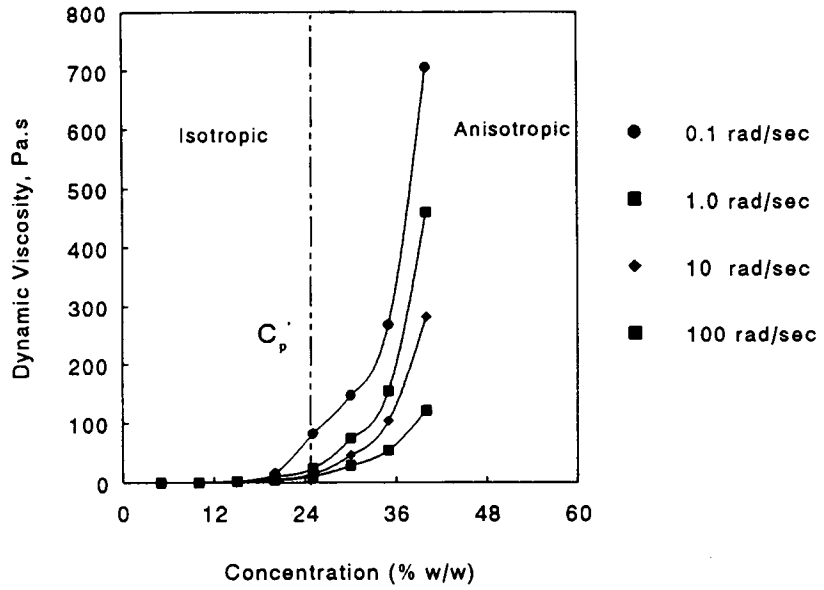

Figure 4 Dynamic viscosity vs. concentration of cellulose hexanoate solutions in DMAc at different frequencies.

40% (w/w) concentration. Since the viscosity measurements (Figs. 4–6) failed to reveal typical liquid crystalline solution behavior, C_p' is in this case defined as the value determined by optical microscopy, i.e., 25% (w/w). This value corresponds to $V_p^c = 0.16$. The lyotropic mesophase formation of cellulose hexanoate has not been reported before. This study reveals that cellulose (derivative) solutions must be observed by optical microscopy in addition to rheology for detecting behavior typical of liquid crystallinity.

III. Theoretical Considerations for the Determination of Critical Volume Fractions (V_p^c)

1. Cellulose

Table II shows the theoretical values of molecular parameters for cellulose and cellulose hexanoate.

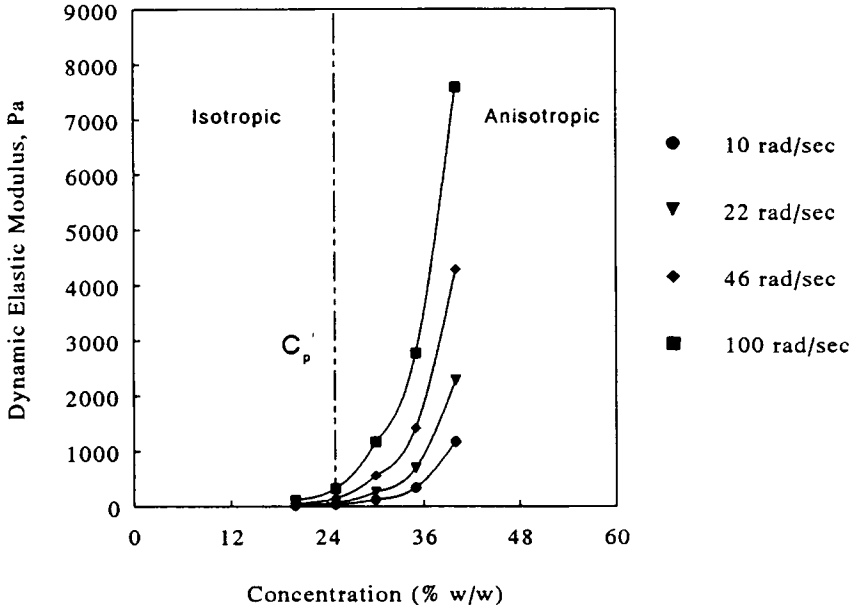

Figure 5 Dynamic elastic modulus vs. concentration of cellulose hexanoate solutions in DMAc at different frequencies.

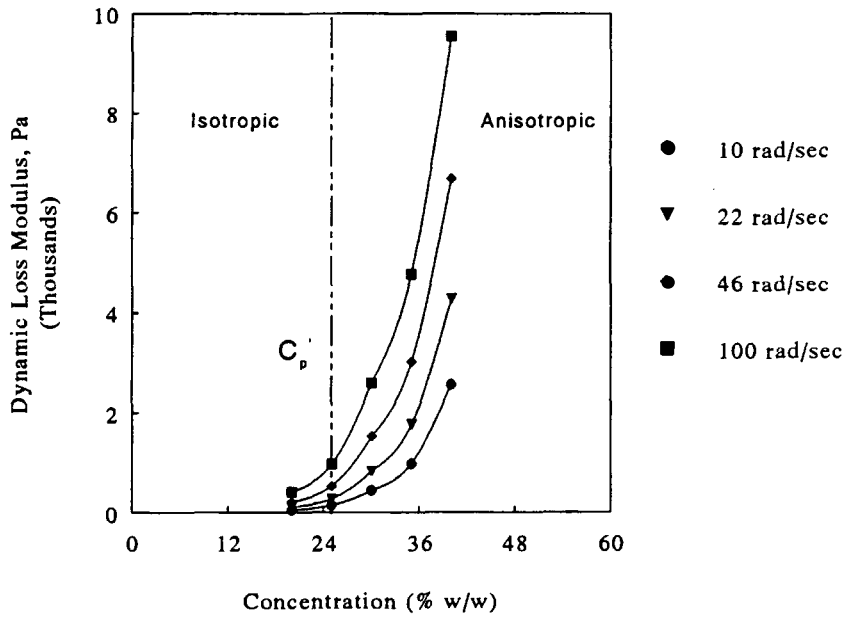

Figure 6 Dynamic loss modulus vs. concentration of cellulose hexanoate solutions in DMAc at different frequencies.

(Please see the Appendix for the calculations.) Flory's lattice theory overestimates the V_p^c value of cellulose in DMAc/LiCl as observed by the deviation between the Kuhn model and experimental data. Such deviations were observed by other investigators in other solvents,[30,41] as well as in DMAc/LiCl.[44,46] The cellulose molecule seems to be stiffened by complexation and association with DMAc/LiCl.[48,49] Presently, there is a lack of careful studies that would allow theoretical treatments of cellulose in ordered phases.

2. Cellulose Hexanoate

The absolute experimental and theoretical values of V_p^c for cellulose hexanoate are in reasonable agreement (Table II). The unsubstituted hydroxyl groups ($DS_{OH} = 2.31$) may form hydrogen bonds and stiffen the backbone. The bulky substituents ($M_u = 229.62$) on the backbone will reduce the hydrogen bonding to a certain extent, but they would contribute to an increase in intermolecular interactions. These two factors may influence the V_p^c in cellulose hexanoate.

IV. Processing

Tables III and IV show the spinning conditions and mechanical properties of the cellulose and cellulose hexanoate fibers. The first column represents the concentration of the solutions from which the fibers were spun. The extrusion rates of the spinning solution, V_0, were 14, 21 and 42 m/min. The values of shear rates to the corresponding V_0 values were 6220, 9330, and 18,660 s^{-1}, respectively. The takeup speed, V_L, varied between 11 and 46 m/min.

A draw ratio of less than 1 reflects die swelling due to the release of stored energy as the solutions were elastic. The draw ratio values are expected to be higher than reported if the velocity of the freely extruded filaments were used instead of V_0. Die swelling was larger for isotropic solutions than for liquid crystalline solutions. A detailed study on die swelling for cellulose solutions was reported by Bianchi et al.[50]

Cellulose solutions were wet spun under a wide range of conditions in comparison to cellulose hexanoate and other cellulose esters like cellulose acetate and cellulose acetate butyrate studied earlier.[55] There was no marked difference in the spinnability of isotropic and liquid crystalline cellulose and cellulose hexanoate solutions.

V. Mechanical Properties

1. Cellulose

Figure 9 represents the modulus variation with spinning dope concentration of cellulose fibers spun at different takeup speeds (only data for $V_0 = 21$ m/min are shown). The modulus values increase

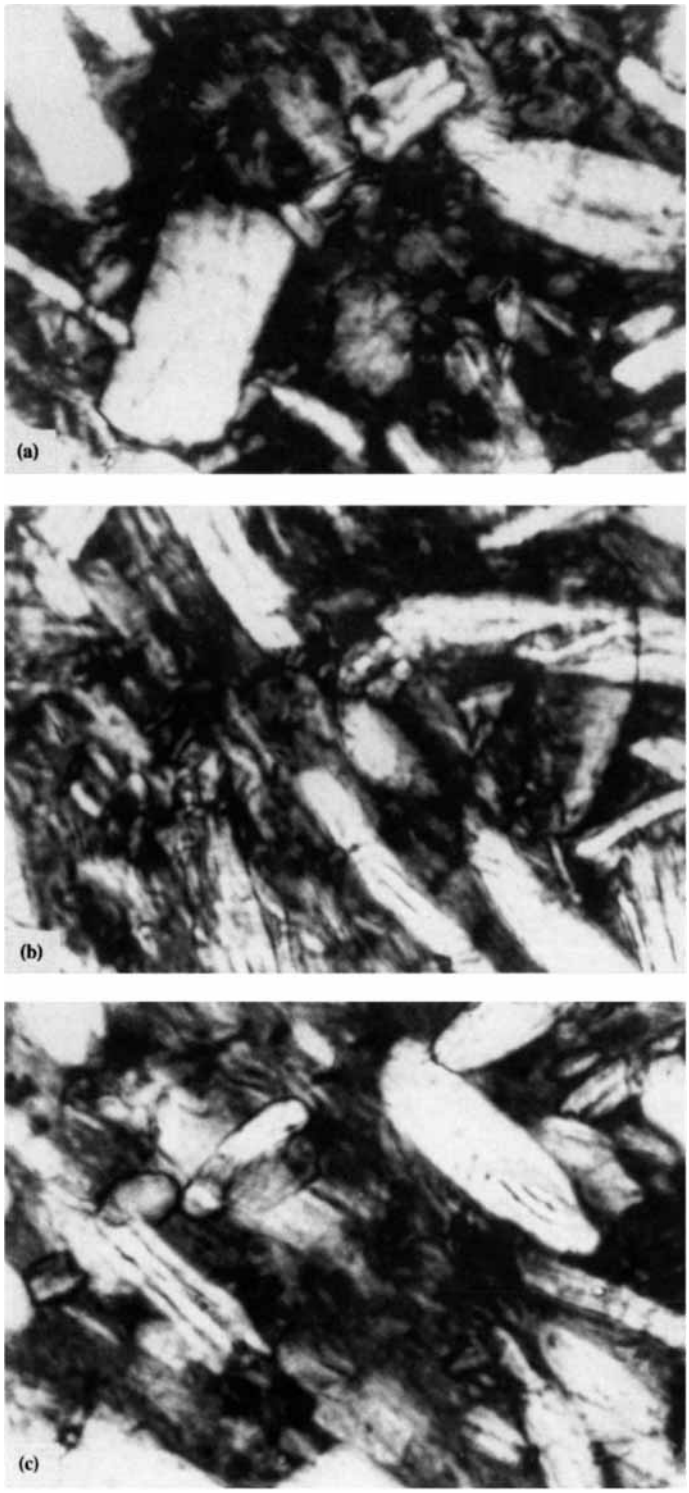

Figure 7 Polarized optical micrographs of cellulose solutions in DMAc/LiCl: (a) 10% (w/w); (b) 12% (w/w); (c) 13.5% (w/w).

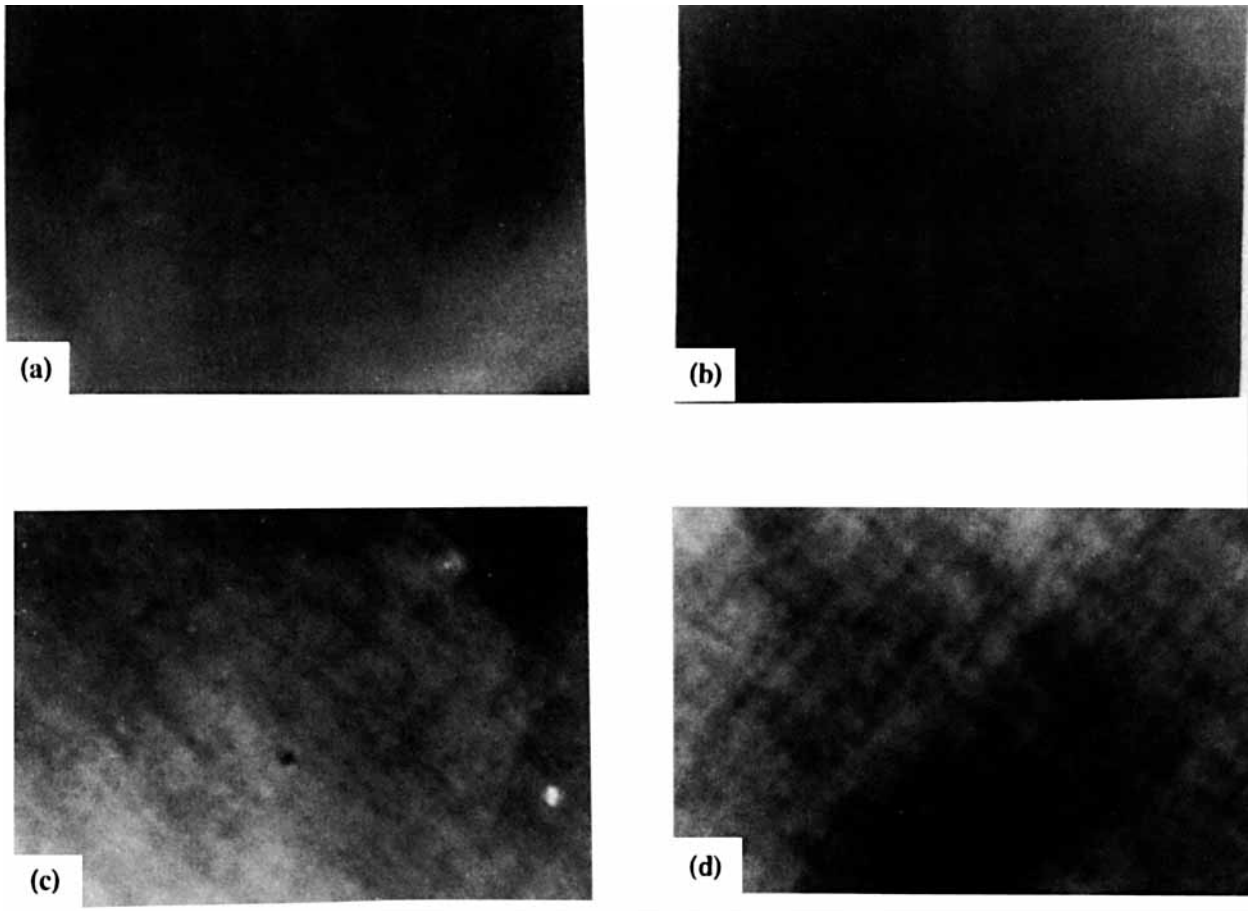

Figure 8 Polarized optical micrographs of cellulose hexanoate solutions in DMAc: (a) 25% (w/w); (b) 30% (w/w); (c) 35% (w/w); (d) 40% (w/w).

for the fibers spun from anisotropic solutions. The modulus values were also higher when the takeup speed was increased. Extrusion rate does not seem to affect the fiber properties as high modulus values, i.e., 119.4 and 115.2 g/d, were obtained from V_0 values of 14 and 21 m/min, respectively, at takeup speeds of 15 m/min. The "dry jet/wet" spinning method allows higher takeup speeds, resulting in higher fiber orientation. The weakening effect caused by high extrusion rates[49,50] was avoided by spinning the fibers at high takeup speeds. Highest modulus and tenacity values obtained in this study were 151.9 g/d (20.8 GPa) and 1.1 g/d (0.15 GPa), respectively, for the cellulose fibers. These values

Table II Theoretical Values of Molecular Parameters for Cellulose (C) and Cellulose Hexanoate (CH)

	ρ (g/cm^3)	M_u (gm/mol)	d (Å)	l_k (Å)	q (Å)	X_K	Theor. V_p^c	Expt V_p^c
C	1.6	162	5.7	250	125	43.86	0.17	0.04[a]
CH	1.6	229.62	6.8	207.7	103.85	30.5	0.24	0.16[b]

[a] Based on viscosity measurements.
[b] Based on polarized optical microscopy observations.

Table III Spinning Conditions and Mechanical Properties of Cellulose Fibers

C_p (w/w %)	Ph	V_0 (m/min)	V_L (m/min)	Draw Ratio[a]	D[b] (μm)	E (g/d)[c]	σ_b (g/d)	ε_b (%)	BT (g/d)
C-6.5	I	14	11	0.80	107	23.9	0.58	1.0	0.02
C-6.5	I	14	15	1.07	95	34.7	0.56	1.1	0.02
C-6.5	I	14	21	1.50	98	79.2	0.75	1.7	0.05
C-6.5	I	21	11	0.52	144	33.8	0.57	1.5	0.02
C-6.5	I	21	21	1.00	137	53.9	0.68	1.0	0.02
C-6.5	I	21	30	1.43	126	58.1	0.97	1.8	0.04
C-6.5	I	21	46	2.20	50	34.4	1.10	1.5	0.07
C-8.0	I	14	11	0.80	128	24.9	0.62	0.7	0.01
C-8.0	I	14	15	1.07	89	50.2	0.73	0.4	0.01
C-8.0	I	14	21	1.50	88	71.0	0.96	1.0	0.05
C-8.0	I	14	30	2.14	81	60.0	0.93	5.8	0.11
C-8.0	I	21	11	0.52	161	67.7	0.88	0.8	0.03
C-8.0	I	21	21	1.00	91	35.6	0.55	0.2	0.02
C-8.0	I	21	30	1.43	86	40.9	0.61	1.5	0.02
C-10.0	B	14	11	0.80	139	108.2	0.74	1.6	0.01
C-10.0	B	14	21	1.50	100	101.2	0.65	1.0	0.01
C-10.0	B	14	30	2.14	91	112.8	1.10	1.0	0.01
C-10.0	B	21	21	1.00	110	70.6	0.71	2.8	0.03
C-10.0	B	21	30	1.43	105	115.3	0.63	2.0	0.02
C-12.0	B	21	15	0.72	144	105.1	0.61	1.5	0.01
C-12.0	B	21	21	1.00	115	110.5	0.42	2.0	0.02
C-12.0	B	21	30	1.43	103	144.1	1.10	2.0	0.02
C-13.5	B	14	11	0.80	180	101.5	0.73	2.4	0.02
C-13.5	B	14	15	1.07	145	119.4	0.82	1.5	0.01
C-13.5	B	21	15	0.72	171	115.2	1.10	2.9	0.02
C-13.5	B	21	21	1.00	151	120.6	0.82	2.9	0.02
C-13.5	B	21	25	1.20	85	151.9	0.85	2.2	0.02

[a] Draw ratio = V_L/V_0.
[b] These fiber diameters were larger by several factors than what is current industry norm. At diameters of < 20 μm, (tensile) properties normally improve considerably. Fibers of such low diameter could not be produced in the current study due to instrumental constraints.
[c] 1 GPa $\approx$ 7.3 g/d.

Table IV Spinning Conditions and Mechanical Properties of Cellulose Hexanoate Fibers

C_p (w/w %)	Ph.[a]	V_0 (m/min)	V_L (m/min)	Draw Ratio[b]	D[c] (μm)	E (g/d)[d]	σ_b (g/d)	ε_b (%)	BT[e] (g/d)
CH-20	I	42	15	0.36	197	22.7	0.4	6	0.01
CH-20	I	42	21	0.50	173	19.4	0.5	16	0.07
CH-20	I	42	35	0.80	151	16.8	0.4	16	0.05
CH-30	B	21	11	0.52	185	15.2	0.5	26	0.11
CH-30	B	21	21	1.00	150	17.8	0.7	25	0.13
CH-30	B	42	21	0.52	190	18.9	0.5	30	0.13
CH-30	B	42	35	0.83	176	22.0	0.5	25	0.10

[a] Ph. represents different phases. I and B designate isotropic and biphasic phases.
[b] Draw ratio = V_L/V_0.
[c] See footnote b to Table III.
[d] 1 GPa $\approx$ 7.3 g/d.
[e] BT = breaking toughness.

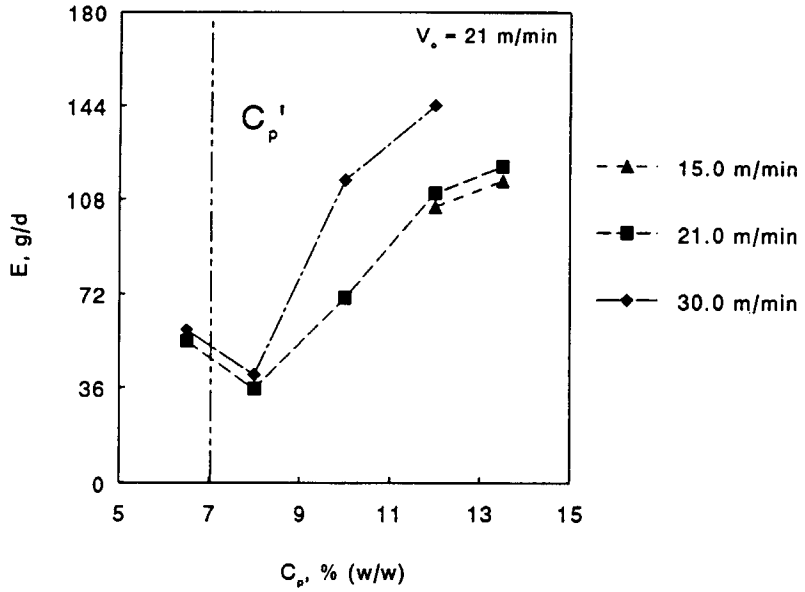

Figure 9 Modulus vs. polymer concentration of cellulose fibers spun at different takeup speeds for V_0 = 21 m/min.

are comparable[27,55] and superior[41] to the cellulose fibers obtained by other investigators. Unlike cellulose derivatives, the solubility limit of cellulose does not allow cellulose solutions to become completely anisotropic. The biphasic liquid crystalline solution state restricts cellulose to reach its maximum mechanical properties. The strength (tenacity) values do not show great improvements at different takeup speeds and different liquid crystalline contents of the solutions. The fiber properties can be further improved by using high molecular weight cellulose and longer maturation and nucleation times of the solutions.

2. *Cellulose Hexanoate*

Figure 10 shows the variation of modulus of cellulose hexanoate fibers on going through the isotropic–anisotropic transition at different takeup speeds for V_0 = 42 m/min. Modulus values do not increase, as expected, possibly due to the coexistence of an isotropic phase in the biphasic liquid crystalline solution. It should be noted that cellulose hexanoate fibers were not spun from completely anisotropic solution concentration, i.e., 40% (w/w). However, the modulus value improved for the fibers spun at takeup speeds of 35 m/min. But the takeup speeds were probably not high enough to compensate for the weakening effect caused by the high extrusion rate (i.e., 42 m/min). No one has yet reported fibers from cellulose hexanoate.

VI. Morphology

Cellulose fibers were slightly tacky immediately after they emerged from the coagulation bath at all takeup speeds. This could be due to complexation and association of DMAc/LiCl with cellulose that may have influenced the coagulation rate.

1. *Cellulose*

Figure 11 shows the scanning electron micrographs of the surfaces of fibers spun from low (6.5%) and high (13.5%) concentration. The fibers from low concentration had smooth surfaces, whereas the fibers from high concentration were rough. Figure 11(b) is the micrograph of a fiber bundle. At low concentrations, more coagulant was needed to diffuse into the solution to precipitate the polymer, and, consequently, this led to a slower coagulation rate. This resulted in a uniform structure. The coagulation rate of higher concentration solutions was faster as less coagulant was required to precipitate the polymer. This resulted in a rougher structure.

2. *Cellulose Hexanoate*

Figure 12 shows the surface morphology of cellulose hexanoate fibers spun from 30% (w/w) solution. (The surface structure of fibers from 20% [w/w] solution was similar to that of 30% [w/w] solution.) The smooth and uniform structure indicates slow coagulation due to relatively low concentration.

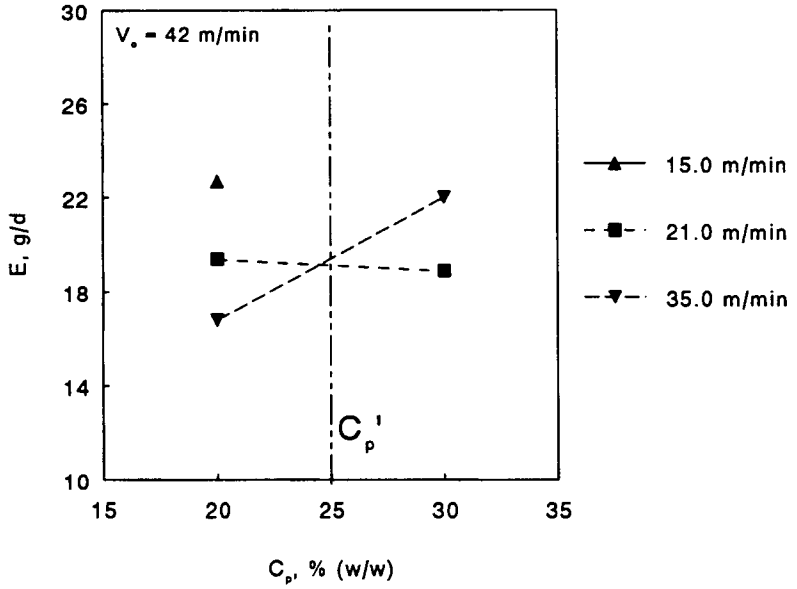

Figure 10 Modulus vs. polymer concentration of cellulose hexanoate fibers spun at different takeup speeds for V_0 = 42 m/min.

Concentration effects on morphology may be observed for fibers spun from higher concentrations.

The cellulose hexanoate examined in this study is expected to (a) retain the properties of cellulose due to its low degree of substitution (DS_{OH} = 0.69) and (b) to exhibit behavior resembling cellulose ester derivatives due to its improved solubility. Derivatization seems to have reduced the hydrogen bonding to some extent as LiCl was not required to dissolve cellulose hexanoate. This is evident as the viscosity of cellulose hexanoate solutions was lower than that of cellulose solutions. However, in contrast to cellulose and cellulose derivatives, the viscosity of cellulose hexanoate solutions did not drop after the onset of liquid crystallinity. This difference in viscosity behavior may be explained by the presence of interactions and associations between the long side-chain substituents of hexanoic acid groups. The extent of these interactions is expected to be relatively lower for derivatives with shorter side chains like cellulose acetate (CA) and cellulose acetate butyrate (CAB). In case of cellulose, CA and CAB, at critical concentration, the viscosity drops as the liquid crystalline order seems to overcome the association between side chains. However, in case of cellulose hexanoate, it seems that extensive side-chain association dominates the liquid crystalline order and inhibits the drop in viscosity. In fact, these side-chain interactions and associations may also be responsible for lowering the critical concentration at which liquid crystalline solutions form for the cellulose esters. The viscosity behavior at high solution concentration of cellulose hexanoate and cellulose is analogous. Unlike cellulose, cellulose hexanoate is highly soluble, and it presumably is not in a metastable condition. Similar to other cellulose derivatives, at high concentrations, packing effects of the cellulose hexanoate molecules may be responsible for the continuing rise in viscosity with concentration.[57]

The experimental value of V_p^c (0.16) of cellulose hexanoate was lower than the cellulose ester with the maximum degree of butyration, CAB-3, studied earlier.[51] The decrease in V_p^c could be due to the bulky hexanoic acid groups that raise intermolecular interaction. However, the comparison may not be justified as cellulose hexanoate has a low *DS* that provides ample opportunity for hydrogen bonding. Our prediction that solution anisotropy can be reached at lower concentrations in cellulose esters with large and bulky substituents seems correct; however, further investigation is required to deconvolute the conflicting effects of substituent size and hydrogen bonding.

The highest modulus and tenacity for cellulose hexanoate fibers achieved in this study is 22.7 and 0.7 g/d, respectively. These values are higher than those obtained from all other fibers produced from isotropic solutions, and they are higher than those of some of the fibers produced from anisotropic solutions of cellulose esters (i.e., CAB) reported earlier.[55] This could be due to the presence of hydrogen

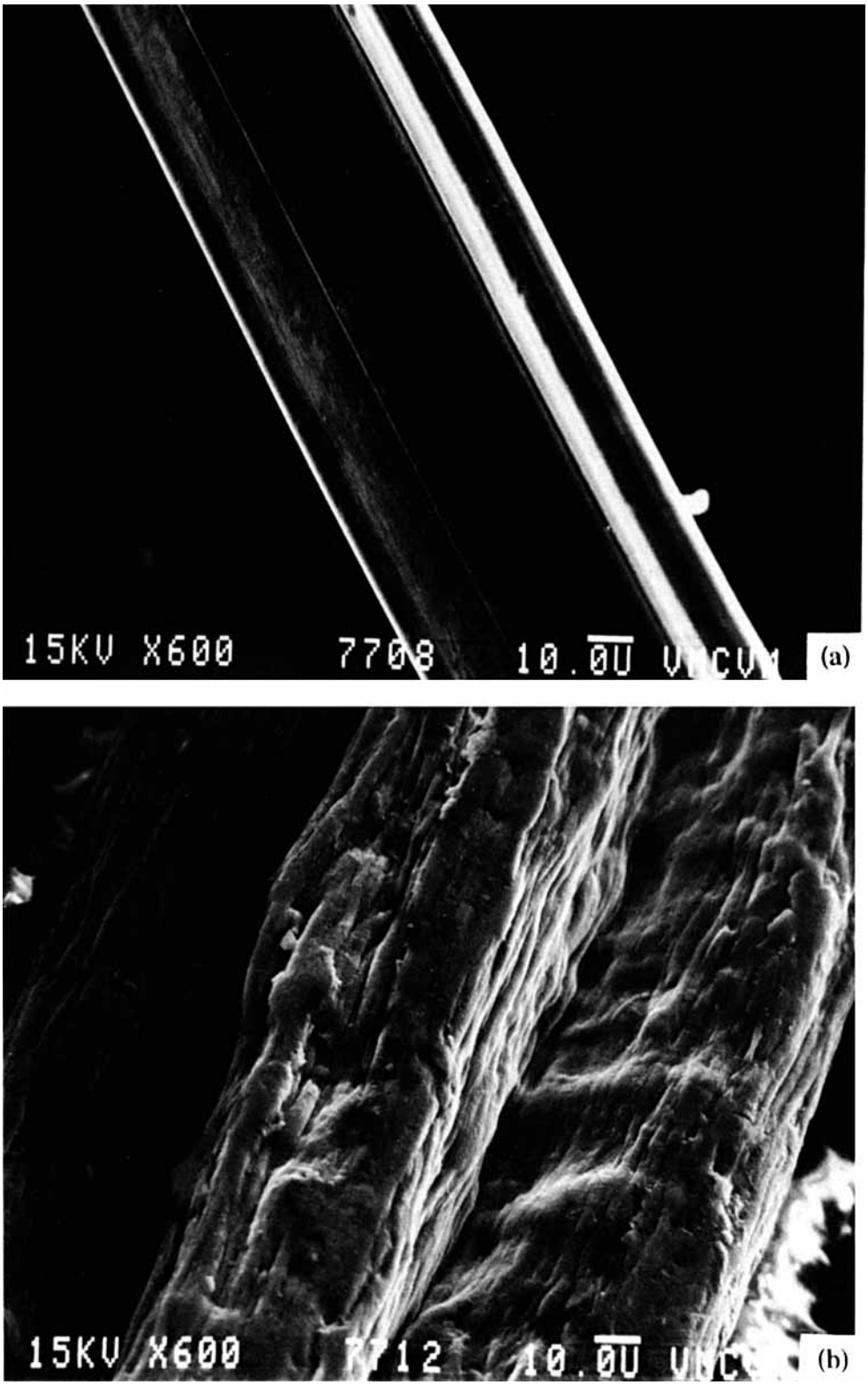

Figure 11 SEM of the surface of cellulose fibers: (a) 6.5% (w/w), V_0 = 14 m/min, V_L = 21 m/min; (b) 13.5% (w/w), V_0 = 21 m/min, V_L = 15 m/min.

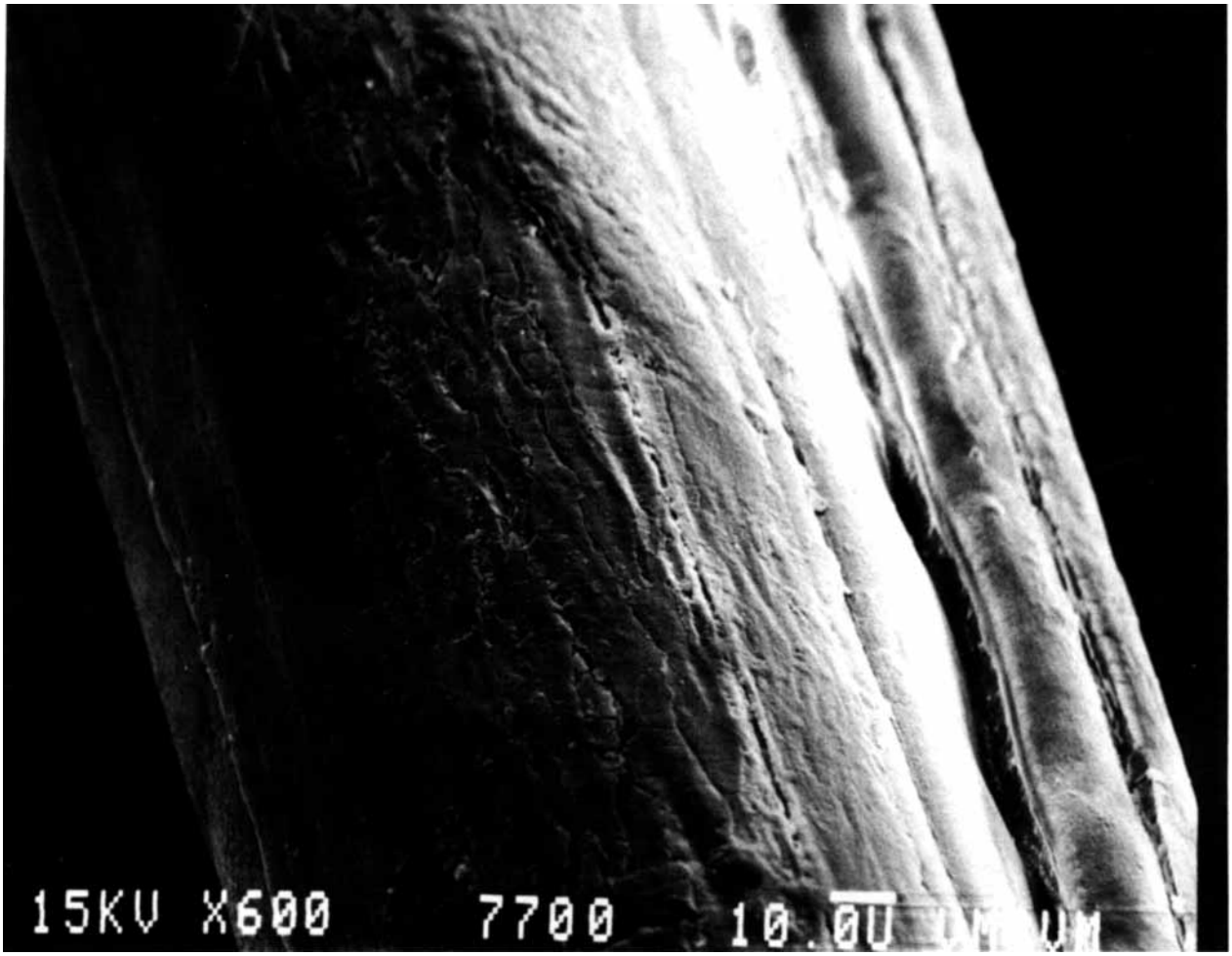

Figure 12 SEM of the surface of cellulose hexanoate fiber spun from 30% (w/w) solution at V_0 = 21 m/min and V_L = 21 m/min.

bonding in cellulose hexanoate. However, these properties are lower than those of cellulose fibers. Therefore, the properties of cellulose hexanoate fibers are in between those of unmodified cellulose and those of completely derivatized cellulose (ester) fibers.

CONCLUSIONS

1. Cellulose and cellulose hexanoate solutions were liquid crystalline above 7% (w/w) and 25% (w/w) concentrations, respectively. Cellulose formed biphasic solutions at all concentrations due to limited solubility, whereas cellulose hexanoate became completely anisotropic (see Fig. 8) at higher concentrations. The viscosity of cellulose solutions resembles typical liquid crystalline behavior. However, the viscosity of cellulose hexanoate solutions did not decrease at the onset of liquid crystalline behavior, possibly because of extensive side-chain interactions.
2. The experimental value of the critical volume fraction, V_p^c, of cellulose hexanoate (0.16) was lower than that of cellulose esters with maximum degree of butyration, CAB-3, (i.e., 0.29) studied earlier.
3. The modulus of the cellulose fibers increased when spun from liquid crystalline solutions. Similar observations were not evident for cellulose hexanoate fibers. This may be explained by the weakening effect of the high extrusion rates applied and of the incomplete development of the liquid crystalline structure at low concentrations.

4. Cellulose fibers spun from low concentration isotropic solutions had a smooth surface morphology, whereas the fibers from high concentration liquid crystalline solutions had a coarse surface structure.

We appreciate the support of this research by the National Science Foundation Science and Technology Center for High Performance Polymeric Adhesives and Composites at Virginia Tech under Contract DMR8809714. The authors would like to thank Dr. Gamini Samaranayake (Wood Science) for providing cellulose hexanoate as well as valuable advice.

APPENDIX A

1. Calculation of molecular weights of repeat units, M_u:
   Cellulose: $M_u = 162$
   Cellulose Hexanoate: $M_u = 162 + 98 \times 0.69 = 229.62$.

2. Calculation of chain diameter, d: $d = (M_u/N_A\rho l_u)^{1/2}$: $l_u = 5.2$ Å, $N_A = 6.02 \times 10^{23}$ molecules/mol.
   Cellulose:
   $d = (162/6.02 \times 10^{23} \times 1.6 \times 10^{-24} \times 5.2)^{1/2} = 5.7$ Å.
   Cellulose hexanoate:
   $d = (229.62/6.02 \times 10^{23} \times 1.6 \times 10^{-24} \times 5.2)^{1/2} = 6.8$ Å.

3. Calculation of Kuhn segment length, l_k: $l_k = \langle r^2 \rangle_0 / nl_u$:
   From light scattering [Tanner and Berry[58]]:
   $\langle rcf112 \rangle_0/n = 1080$ Å^2.
   A narrow range of values of $\langle r^2 \rangle_0/n$ have been reported for diverse cellulose esters;[58] therefore, 1080 Å^2 is assumed for cellulose hexanoate in this study:
   $l_k = 1080/5.2 = 207.7$ Å.

4. Calculation of persistence length, q: $q = l_k/2$:
   Cellulose: $q = 125$ Å (Ref. 49)
   Cellulose hexanoate: $q = 207.7/2 = 103.85$ Å.

5. Calculation of aspect ratio, $X_k = 2q/d$:
   Cellulose: $X_k = 2 \times 125/5.7 = 43.86$
   Cellulose hexanoate: $X_k = 2 \times 103.85/6.8 = 30.5$.

6. Calculation of critical concentration, V_p^c:
   Cellulose: $V_p^c = 8/43.86(1 - 2/43.86) = 0.17$
   Cellulose hexanoate: $V_p^c = 8/30.5(1 - 2/30.5) = 0.24$.

REFERENCES

1. D. M. MacDonald, in *Solvent Spun Rayon, Modified Cellulose Fibers and Derivatives,* A. F. Turbak, Ed., ACS Symposium Series 58, American Chemical Society, Washington, DC, 1977, pp. 25–39.
2. R. B. Hammer and A. F. Turbak, in *Solvent Spun Rayon, Modified Cellulose Fibers and Derivatives,* A. F. Turbak, Ed., ACS Symposium Series 58, American Chemical Society, Washington, DC, 1977, pp. 44–51.
3. D. C. Johnson, M. D. Nicholson, and F. C. Haigh, *Appl. Polym. Symp.,* **28,** 931 (1976).
4. K. Kamide, K. Okajima, T. Matsui, and S. Manabe, *Polym. J. (Tokyo),* **12,** 521 (1980).
5. O. Turunen, L. Mandell, V. Eklund, K. Ekman, and J. Huttunen, U.S. Pat. 4,486,585 (1984).
6. S. M. Hudson and J. A. Cuculo, *J. Macromol. Sci. Rev. Macromol. Chem.,* **C18**(1), 1–82 (1980).
7. C. Graenacher and R. Sallman, U.S. Pat. 2,179,181 (1939).
8. D. L. Johnson, U.S. Pat. 3,447,939 (1969).
9. N. E. Franks and J. K. Varga, U.S. Pat. 4,145,532 (1979).
10. C. C. McCorsley and J. K. Varga, U.S. Pat. 4,142,913 (1979).
11. C. C. McCorsley, U.S. Pat. 4,144,080 (1979).
12. C. C. McCorsley and J. K. Varga, U.S. Pat. 4,211,574 (1980).
13. R. N. Armstrong, C. C. McCorsley, and J. K. Varga, in *Proceedings of the Fifth International Tappi Pulp Conference,* Vienna, 1980, p. 100.
14. C. C. McCorsley, U.S. Pat. 4,246,221 (1981).
15. H. Chanzy, A. Peguy, S. Chaunis, and P. Monzie, *J. Polym. Sci. Polym. Phys. Ed.,* **18,** 1137–1144 (1980).
16. E. Maia, A. Peguy, and S. Perez, *Acta Crystallogr. B,* **37,** 1858–1862 (1981).
17. E. Maia and S. Perez, *Acta Crystallogr. B,* **38,** 849–852 (1982).
18. H. Chanzy, E. Maia, and S. Perez, *Acta Crystallogr. B,* **38,** 852–855 (1982).
19. K. Okamura, M. Fujita, and T. Umezawa, *Bull. Kyoto Univ. Forests,* **53**(11), 254 (1981).
20. P. Navard and J. M. Haudin, *Br. Polym. J.,* **12,** 174–178 (1980).
21. P. Navard and J. M. Haudin, *Polym. Proc. Eng.,* **3**(3), 291–301 (1985).
22. H. Chanzy, P. Noe, M. Paillet, and P. Smith, *J. Appl. Polym. Sci.,* **37,** 239–259 (1983).
23. H. Chanzy, M. Dube, and R. H. Marchessault, *J. Polym. Sci. Polym. Lett. Ed.,* **17,** 219–226 (1979).
24. H. Chanzy, S. Nawrot, A. Peguy, P. Smith, and J. Chevalier, *J. Polym. Sci. Polym. Phys. Ed.,* **20,** 1909–1924 (1982).
25. H. Chanzy, A. Peguy, S. Chaunis, and P. Monzie, *Proceedings of the Fifth International Tappi Dissl. Pulp Conference,* Vienna, 1980, pp. 105–108.

26. H. Chanzy, S. Nawrot, S. Perez, and P. Smith, *Proceedings of International Tappi Dissl. Pulp Conference,* Atlanta, 1983, pp. 127–132.
27. H. Chanzy, M. Paillet, and R. Hagege, *Polymer,* **30**(3), 400–405 (1990).
28. H. Chanzy, B. Chumpitazi, and A. Peguy, *Carbohyd. Polym.,* **2,** 35–42 (1982).
29. D. L. Patel and R. D. Gilbert, *J. Polym. Sci. Polym. Phys. Ed.,* **19,** 1231–1236 (1981).
30. Y. K. Hong, D. E. Hawkinson, E. Kohout, A. Garrard, R. E. Fornes, and R. D. Gilbert, in *Polymer Association Structures,* M. A. El-Nokaly, Ed., ACS Symposium Series 384, American Chemical Society, Washington, DC, 1989, pp. 184–203.
31. V. V. Myasoedova, O. A. Adamova, and G. A. Krestov, *Vysokomol. Soedin Ser. B,* **26**(3), 215 (1984).
32. S. P. Papkov, Y. Y. Belousov, and V. E. Kulichikhin, *Khim. Volokna,* **3,** 8 (1983).
33. V. V. Myasoedova, O. V. Alekseeva, and G. A. Krestov, *Zh. Prikl. Khim. (Leningrad),* **60**(10), 2526 (1987).
34. P. Scherer, *J. Am. Chem. Soc.,* **53,** 4009 (1931).
35. S. M. Hudson and J. A. Cuculo, *J. Polym. Sci. Polym. Chem. Ed.,* **18,** 3469–3481 (1980).
36. J. A. Cuculo and S. M. Hudson, U.S. Pat. 4,367,191 (1983).
37. S. M. Hudson, J. A. Cuculo, and L. C. Wadsworth, *J. Polym. Sci. Polym. Chem. Ed.,* **21,** 651 (1983).
38. C. K. Liu, J. A. Cuculo, and B. Smith, *J. Polym. Sci. Part B Polym. Phys.,* **27,** 2493–2511 (1989).
39. J. J. Cho, S. M. Hudson, and J. A. Cuculo, *J. Polym. Sci. Part B Polym. Phys.,* **27,** 1699–1719 (1989).
40. C. K. Liu, J. A. Cuculo, and B. Smith, *J. Polym. Sci. Part B Polym. Phys.,* **28,** 449–465 (1990).
41. K. S. Yang, M. H. Theil, and J. A. Cuculo, in *Polymer Association Structures,* M. A. El-Nokaly, Ed., ACS Symposium Series 384, American Chemical Society, Washington, DC, 1989, pp. 156–183.
42. C. L. McCormick, U.S. Pat. 4,278,790 (1981).
43. C. L. McCormick and P. A. Callais, *Polymer,* **28,** 2317–2323 (1987).
44. C. L. McCormick, P. A. Callais, and B. H. Hutchinson, Jr., *Macromolecules,* **18**(12), 2394–2401 (1985).
45. C. L. McCormick, P. A. Callais, and B. H. Hutchinson, Jr., *Polym. Prepr. (ACS Div. Polym. Chem.),* **24**(2), 271 (1983).
46. G. Conio, P. Corazza, E. Bianchi, A. Tealdi, and A. Ciferri, *J. Polym. Sci. Polym. Lett. Ed.,* **22,** 273–277 (1984).
47. A. F. Turbak, A. Kafraw, F. Synder, and A. Auerback, U.S. Pats. 4,302,252 (1981) and 4,352,770 (1982).
48. M. Terbojevich, A. Cosani, G. Conio, A. Ciferri, and E. Bianchi, *Macromolecules,* **18,** 640–646 (1985).
49. E. Bianchi, A. Ciferri, G. Conio, A. Cosani, and M. Terbojevich, *Macromolecules,* **18,** 646–650 (1985).
50. E. Bianchi, A. Ciferri, G. Conio, A. Cosani, and A. Tealdi, *J. Polym. Sci. Part B Polym. Phys.,* **27,** 1477–1484 (1989).
51. V. Davé and W. G. Glasser, in *Viscoelasticity of Biomaterials,* W. G. Glasser and H. Hatakeyama, Eds. ACS Symposium Series 489, American Chemical Society, Washington, DC, 1992, pp. 144–165.
52. G. Samaranayake and W. G. Glasser, to appear.
53. R. Evans and A. F. A. Wallis, in *Fourth International Symposium on Wood and Pulping Chemistry,* Paris, Vol. 1, pp. 201–205. 1987.
54. C. L. McCormick and T. S. Chen, in *Macromolecular Solutions,* R. B. Seymour and G. A. Stahl, Eds., Pergamon Press, New York, 1982.
55. V. Davé, W. G. Glasser, and G. L. Wilkes, to appear.
56. R. B. Bird, R. C. Armstrong, and O. Hassager, in *Dynamics of Polymeric Liquids,* Vol. 1, 2nd edition, John Wiley and Sons, New York, 1987, p. 150.
57. S. Dayan, J. M. Gilli, and P. Sixou, *J. Appl. Polym. Sci.,* **28,** 1527 (1983).
58. W. D. Tanner and G. C. Berry, *J. Polym. Sci. Polym. Phys. Ed.,* **12,** 941 (1974).

Received April 27, 1992
Accepted August 3, 1992